

## CHAPTER ONE

---

# INTRODUCTION

### 1.1 NONLINEAR COMPUTATIONAL MECHANICS

Two sources of nonlinearity exist in the analysis of solid continua, namely, material and geometric nonlinearity. The former occurs when, for whatever reason, the stress–strain behavior given by the constitutive relation is nonlinear, whereas the latter is important when changes in geometry, however large or small, have a significant effect on the load deformation behavior. Material nonlinearity can be considered to encompass contact friction, whereas geometric nonlinearity includes deformation-dependent boundary conditions and loading.

Despite the obvious success of the assumption of linearity in engineering analysis, it is equally obvious that many situations demand consideration of nonlinear behavior. For example, ultimate load analysis of structures involves material nonlinearity and perhaps geometric nonlinearity, and any metal-forming analysis such as forging or crash-worthiness must include both aspects of nonlinearity. Structural instability is inherently a geometric nonlinear phenomenon, as is the behavior of tension structures. Indeed the mechanical behavior of the human body itself, say in impact analysis, involves both types of nonlinearity. Nonlinear and linear continuum mechanics deal with the same subjects, including kinematics, stress and equilibrium, and constitutive behavior. But in the linear case an assumption is made that the deformation is sufficiently small to enable the effect of changes in the geometrical configuration of the solid to be ignored, whereas in the nonlinear case the magnitude of the deformation is unrestricted.

Practical stress analysis of solids and structures is unlikely to be served by classical methods, and currently numerical analysis, predominately in the form of the finite element method, is the only route by which the behavior of a complex component subject to complex loading can be successfully simulated. The study of the numerical analysis of nonlinear continua using a computer is called *nonlinear computational mechanics*, which, when applied specifically to the investigation of solid

continua, comprises nonlinear continuum mechanics together with the numerical schemes for solving the resulting governing equations.

The finite element method may be summarized as follows. It is a procedure whereby the continuum behavior described at an infinity of points is approximated in terms of a finite number of points, called *nodes*, located at specific points in the continuum. These nodes are used to define regions, called *finite elements*, over which both the geometry and the primary variables in the governing equations are approximated. For example, in the stress analysis of a solid the finite element could be a tetrahedron defined by four nodes and the primary variables the three displacements in the Cartesian directions. The governing equations describing the nonlinear behavior of the solid are usually recast in a so-called *weak integral form* using, for example, the principle of virtual work or the principle of stationary total potential energy. The finite element approximations are then introduced into these integral equations, and a standard textbook manipulation yields a finite set of nonlinear algebraic equations in the primary variable. These equations are then usually solved using the Newton–Raphson iterative technique.

The topic of this book can succinctly be stated as the exposition of the nonlinear continuum mechanics necessary to develop the governing equations in continuous and discrete form and the formulation of the Jacobian or tangent matrix used in the Newton–Raphson solution of the resulting finite set of nonlinear algebraic equations.

## 1.2 SIMPLE EXAMPLES OF NONLINEAR STRUCTURAL BEHAVIOR

It is often the case that nonlinear behavior concurs with one’s intuitive expectation of the behavior and that it is linear analysis that can yield the nonsensical result. The following simple examples illustrate this point and provide a gentle introduction to some aspects of nonlinear behavior. These two examples consider rigid materials, but the structures undergo finite displacements; consequently, they are classified as geometrically nonlinear problems.

### 1.2.1 Cantilever

Consider the weightless rigid bar–linear elastic torsion spring model of a cantilever shown in Figure 1.1. Taking moments about the hinge gives the equilibrium equation as

$$FL \cos \theta = M. \quad (1.1)$$

1.2 EXAMPLES OF NONLINEAR STRUCTURAL BEHAVIOR

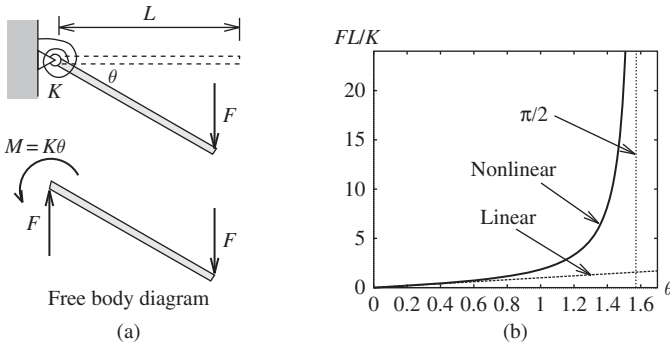


FIGURE 1.1 Simple cantilever.

If  $K$  is the torsional stiffness of the spring, then  $M = K\theta$  and we obtain the following nonlinear relationship between  $F$  and  $\theta$ :

$$\frac{FL}{K} = \frac{\theta}{\cos \theta}. \tag{1.2}$$

If the angle  $\theta \rightarrow 0$ , then  $\cos \theta \rightarrow 1$ , and the linear equilibrium equation is recovered as

$$F = \frac{K}{L}\theta. \tag{1.3}$$

The exact nonlinear equilibrium path is shown in Figure 1.1(b), where clearly the nonlinear solution makes physical sense because  $\theta < \pi/2$ .

1.2.2 Column

The same bar–spring system is now positioned vertically (Figure 1.2(a)), and again moment equilibrium about the hinge gives

$$PL \sin \theta = M \quad \text{or} \quad \frac{PL}{K} = \frac{\theta}{\sin \theta}. \tag{1.4}$$

The above equilibrium equation can have two solutions: first, if  $\theta = 0$  then  $\sin \theta = 0$ ,  $M = 0$ , and equilibrium is satisfied; and second, if  $\theta \neq 0$  then  $PL/K = \theta/\sin \theta$ . These two solutions are shown in Figure 1.2(b), where the vertical axis is the equilibrium path for  $\theta = 0$  and the horseshoe-shaped equilibrium path is the second solution. The intersection of the two solutions is called a *bifurcation point*. Observe that for  $PL/K < 1$  there is only one solution, namely  $\theta = 0$ , but for  $PL/K > 1$  there are three solutions. For instance, when  $PL/K \approx 1.57$ , either  $\theta = 0$  or  $\pm\pi/2$ .

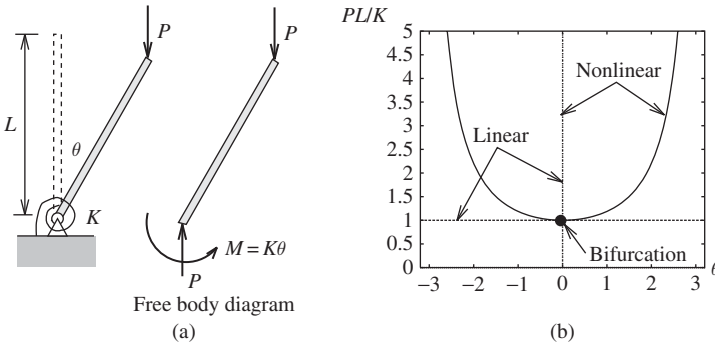


FIGURE 1.2 Simple column.

For very small values of  $\theta$ ,  $\sin \theta \rightarrow \theta$  and Equation (1.4) reduces to the linear (in  $\theta$ ) equation

$$(K - PL)\theta = 0. \tag{1.5}$$

Again there are two solutions:  $\theta = 0$  or  $PL/K = 1$  for any value of  $\theta$ , the latter solution being the horizontal path shown in Figure 1.2(b). Equation (1.5) is a typical *linear stability analysis* where  $P = K/L$  is the elastic critical (buckling) load. Applied to a beam column, such a geometrically nonlinear analysis would yield the Euler buckling load. In a finite element context for, say, plates and shells, this would result in an eigenvalue analysis, the eigenvalues being the buckling loads and the eigenvectors being the corresponding buckling modes.

Observe in these two cases that it is only by considering the finite displacement of the structures that a complete nonlinear solution has been achieved.

### 1.3 NONLINEAR STRAIN MEASURES

In the examples presented in the previous section, the beam or column remained rigid during the deformation. In general, structural components or continuum bodies will exhibit large strains when undergoing a geometrically nonlinear deformation process. As an introduction to the different ways in which these large strains can be measured we consider first a one-dimensional truss element and a simple example involving this type of structural component undergoing large displacements and large strains. We will then give a brief introduction to the difficulties involved in the definition of correct large strain measures in continuum situations.

#### 1.3.1 One-Dimensional Strain Measures

Imagine that we have a truss member of initial length  $L$  and area  $A$  that is stretched to a final length  $l$  and area  $a$  as shown in Figure 1.3. The simplest possible quantity

1.3 NONLINEAR STRAIN MEASURES

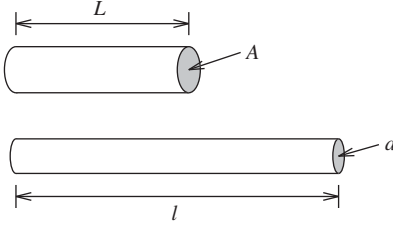


FIGURE 1.3 One-dimensional strain.

that we can use to measure the strain in the bar is the so-called *engineering strain*  $\varepsilon_E$ , defined as

$$\varepsilon_E = \frac{l - L}{L}. \tag{1.6}$$

Clearly different measures of strain could be used. For instance, the change in length  $\Delta l = l - L$  could be divided by the final length rather than the initial length. Whichever definition is used, if  $l \approx L$  the small strain quantity  $\varepsilon = \Delta l/l$  is recovered.

An alternative large strain measure can be obtained by adding up all the small strain increments that take place when the rod is continuously stretched from its original length  $L$  to its final length  $l$ . This integration process leads to the definition of the *natural* or *logarithmic strain*  $\varepsilon_L$  as

$$\varepsilon_L = \int_L^l \frac{dl}{l} = \ln \frac{l}{L}. \tag{1.7}$$

Although the above strain definitions can in fact be extrapolated to the deformation of a three-dimensional continuum body, this generalization process is complex and computationally costly. Strain measures that are much more readily generalized to continuum cases are the so-called *Green* or *Green's strain*  $\varepsilon_G$  and the *Almansi strain*  $\varepsilon_A$ , defined as

$$\varepsilon_G = \frac{l^2 - L^2}{2L^2}; \tag{1.8a}$$

$$\varepsilon_A = \frac{l^2 - L^2}{2l^2}. \tag{1.8b}$$

Irrespective of which strain definition is used, a simple Taylor's series analysis shows that, for the case where  $l \approx L$ , all the above quantities converge to the small strain definition  $\Delta l/l$ . For instance, in the Green strain case, we have

$$\begin{aligned} \varepsilon_G(l \approx L) &\approx \frac{(l + \Delta l)^2 - l^2}{2l^2} \\ &= \frac{1}{2} \frac{l^2 + \Delta l^2 + 2l\Delta l - l^2}{l^2} \\ &\approx \frac{\Delta l}{l}. \end{aligned} \tag{1.9}$$

### 1.3.2 Nonlinear Truss Example

This example is included in order to introduce a number of features associated with finite deformation analysis. Later, in Section 1.4, a small MATLAB program will be given to solve the nonlinear equilibrium equation that results from the truss analysis. The structure of this program is, in effect, a prototype of the general finite element program presented later in this book.

We consider the truss member shown in Figure 1.4 with initial and loaded lengths, cross-sectional areas, and volumes:  $L, A, V$  and  $l, a, v$  respectively. For simplicity we assume that the material is incompressible and hence  $V = v$  or  $AL = al$ . Two constitutive equations are chosen, based, without explanation at the moment, on Green’s and a logarithmic definition of strain, hence the Cauchy, or true, stress  $\sigma$  is either

$$\sigma = E \frac{l^2 - L^2}{2L^2} \quad \text{or} \quad \sigma = E \ln \frac{l}{L}, \tag{1.10a,b}$$

where  $E$  is a (Young’s modulus-like) constitutive constant that, in ignorance, has been chosen to be the same irrespective of the strain measure being used. Physically this is obviously wrong, but it will be shown below that for small strains it is acceptable. Indeed, it will be seen in Chapter 5 that the Cauchy stress cannot be simply associated with Green’s strain, but for now such complications will be ignored.

The equation for vertical equilibrium at the sliding joint  $B$ , in nomenclature that will be used later, is simply

$$R(x) = T(x) - F = 0; \quad T = \sigma a \sin \theta; \quad \sin \theta = \frac{x}{l}; \tag{1.11a,b,c}$$

where  $T(x)$  is the vertical component, at  $B$ , of the internal force in the truss member and  $x$  gives the truss position.  $R(x)$  is the *residual* or *out-of-balance* force,

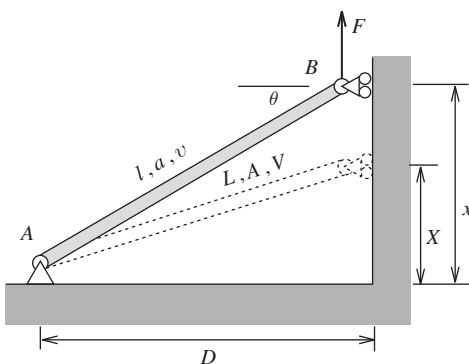


FIGURE 1.4 Single incompressible truss member.

1.3 NONLINEAR STRAIN MEASURES

and a solution for  $x$  is achieved when  $R(x) = 0$ . In terms of the alternative strain measures,  $T$  is

$$T = \frac{Evx}{l^2} \left( \frac{l^2 - L^2}{2L^2} \right) \quad \text{or} \quad T = \frac{Evx}{l^2} \ln \frac{l}{L}. \tag{1.12a,b}$$

Note that in this equation  $l$  is function of  $x$  as  $l^2 = D^2 + x^2$  and therefore  $T$  is highly nonlinear in  $x$ .

Given a value of the external load  $F$ , the procedure that will eventually be used to solve for the unknown position  $x$  is the Newton–Raphson method, but in this one-degree-of-freedom case it is easier to choose a value for  $x$  and find the corresponding load  $F$ . Typical results are shown in Figure 1.5, where an initial angle of  $45^\circ$  has been assumed. It is clear from this figure that the behavior is highly nonlinear. Evidently, where finite deformations are involved it appears as though care has to be exercised in defining the constitutive relations because different strain choices will lead to different solutions. But, at least in the region where  $x$  is in the neighborhood of its initial value  $X$  and strains are likely to be small, the equilibrium paths are close.

In Figure 1.5 the local maximum and minimum forces  $F$  occur at the so-called *limit points*  $p$  and  $q$ , although in reality if the truss were compressed to point  $p$  it would experience a violent movement or *snap-through behavior* from  $p$  to point  $p'$  as an attempt is made to increase the compressive load in the truss beyond the limit point.

By making the truss member initially vertical we can examine the large strain behavior of a rod. The typical load deflection behavior is shown in Figure 1.6, where clearly the same constant  $E$  should not have been used to represent the same material characterized using different strain measures. Alternatively, by making the

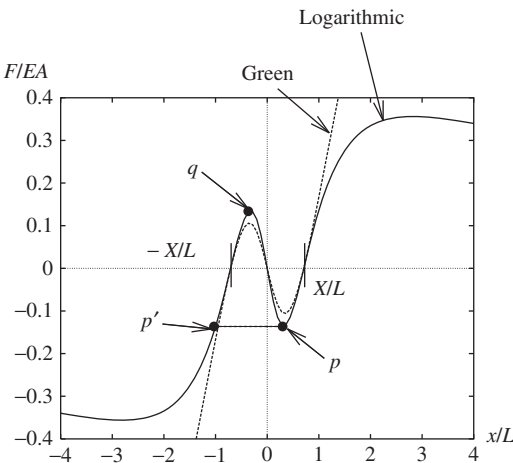


FIGURE 1.5 Truss example – load deflection behavior.

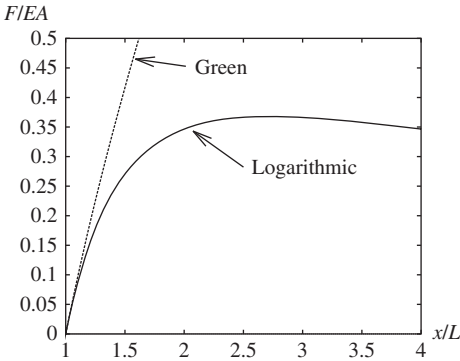


FIGURE 1.6 Large strain rod – load deflection behavior.

truss member initially horizontal, the stiffening effect due to the development of tension in the member can be observed in Figure 1.7.

Further insight into the nature of nonlinearity in the presence of large deformation can be revealed by this simple example if we consider the vertical stiffness of the truss member at joint  $B$ . This stiffness is the change in the equilibrium equation,  $R(x) = 0$ , due to a change in position  $x$ , and is generally represented by  $K = dR/dx$ . If the load  $F$  is constant, the stiffness is the change in the vertical component,  $T$ , of the internal force, which can be obtained with the help of Equations (1.11b,c) together with the incompressibility condition  $a = V/l$  as

$$\begin{aligned} K &= \frac{dT}{dx} \\ &= \frac{d}{dx} \left( \frac{\sigma V x}{l^2} \right) \\ &= \left( \frac{ax}{l} \frac{d\sigma}{dl} - \frac{2\sigma ax}{l^2} \right) \frac{dl}{dx} + \frac{\sigma a}{l} \end{aligned}$$

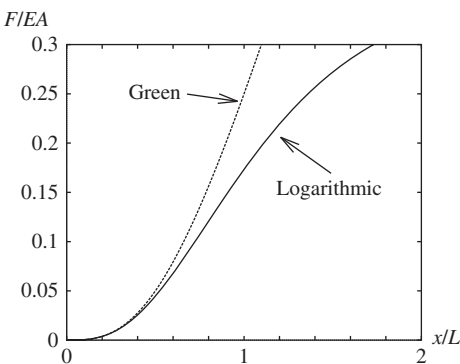


FIGURE 1.7 Horizontal truss – tension stiffening.



1.3 NONLINEAR STRAIN MEASURES

$$= a \left( \frac{d\sigma}{dl} - \frac{2\sigma}{l} \right) \frac{x^2}{l^2} + \frac{\sigma a}{l}. \tag{1.13}$$

All that remains is to find  $d\sigma/dl$  for each strain definition, labeled  $G$  and  $L$  for Green’s and the logarithmic strain respectively, to give

$$\left( \frac{d\sigma}{dl} \right)_G = \frac{El}{L^2} \quad \text{and} \quad \left( \frac{d\sigma}{dl} \right)_L = \frac{E}{l}. \tag{1.14a,b}$$

Hence the stiffnesses are

$$K_G = \frac{A}{L} \left( E - 2\sigma \frac{L^2}{l^2} \right) \frac{x^2}{l^2} + \frac{\sigma a}{l}; \tag{1.15a}$$

$$K_L = \frac{a}{l} (E - 2\sigma) \frac{x^2}{l^2} + \frac{\sigma a}{l}. \tag{1.15b}$$

Despite the similarities in the expressions for  $K_G$  and  $K_L$ , the gradient of the curves in Figure 1.5 shows that the stiffnesses are generally not the same. This is to be expected, again, because of the casual application of the constitutive relations.

Finally, it is instructive to attempt to rewrite the final term in (1.15a) in an alternative form to give  $K_G$  as

$$K_G = \frac{A}{L} (E - 2S) \frac{x^2}{l^2} + \frac{SA}{L}; \quad S = \sigma \frac{L^2}{l^2}. \tag{1.15c}$$

The above expression introduces the second Piola–Kirchhoff stress  $S$ , which gives the force per unit undeformed area but transformed by what will become known as the *deformation gradient inverse*, that is,  $(l/L)^{-1}$ . It will be shown in Chapter 5 that the second Piola–Kirchhoff stress is associated with Green’s strain and not the Cauchy stress, as was erroneously assumed in Equation (1.10a,b)<sub>a</sub>. Allowing for the local-to-global force transformation implied by  $(x/l)^2$ , Equations (1.15c) illustrate that the stiffness can be expressed in terms of the initial undeformed configuration or the current deformed configuration.

The above stiffness terms show that, in both cases, the constitutive constant  $E$  has been modified by the current state of stress  $\sigma$  or  $S$ . We can see that this is a consequence of allowing for geometry changes in the formulation by observing that the  $2\sigma$  term emerges from the derivative of the term  $1/l^2$  in Equation (1.13). If  $x$  is close to the initial configuration  $X$  then  $a \approx A$ ,  $l \approx L$ , and therefore  $K_L \approx K_G$ .

Equations (1.15) contain a stiffness term  $\sigma a/l$  ( $=SA/L$ ) which is generally known as the *initial stress stiffness*. The same term can be derived by considering the change in the equilibrating global end forces occurring when an initially stressed rod rotates by a small amount, hence  $\sigma a/l$  is also called the *geometric stiffness*. This is the term that, in general, occurs in an instability analysis because a sufficiently large negative value can render the overall stiffness singular. The geometric stiffness is unrelated to the change in cross-sectional area and is purely associated with force changes caused by rigid body rotation.

The second Piola–Kirchhoff stress will reappear in Chapter 5, and the modification of the constitutive parameters by the current state of stress will reappear in Chapter 6, which deals with constitutive behavior in the presence of finite deformation.

### 1.3.3 Continuum Strain Measures

In linear stress–strain analysis the deformation of a continuum body is measured in terms of the small strain tensor  $\varepsilon$ . For instance, in a simple two-dimensional case  $\varepsilon$  has components  $\varepsilon_{xx}$ ,  $\varepsilon_{yy}$ , and  $\varepsilon_{xy} = \varepsilon_{yx}$ , which are obtained in terms of the  $x$  and  $y$  components of the displacement of the body as

$$\varepsilon_{xx} = \frac{\partial u_x}{\partial x}; \quad (1.16a)$$

$$\varepsilon_{yy} = \frac{\partial u_y}{\partial y}; \quad (1.16b)$$

$$\varepsilon_{xy} = \frac{1}{2} \left( \frac{\partial u_x}{\partial y} + \frac{\partial u_y}{\partial x} \right). \quad (1.16c)$$

These equations rely on the assumption that the displacements  $u_x$  and  $u_y$  are very small, so that the initial and final positions of a given particle are practically the same. When the displacements are large, however, this is no longer the case and one must distinguish between initial and final coordinates of particles. This is typically done by using capital letters  $X, Y$  for the initial positions and lower-case  $x, y$  for the current coordinates. It would then be tempting to extend the use of the above equations to the nonlinear case by simply replacing derivatives with respect to  $x$  and  $y$  by their corresponding initial coordinates  $X, Y$ . It is easy to show that, for large displacement situations this would result in strains that contradict the physical reality. Consider for instance a two-dimensional solid undergoing a  $90^\circ$  rotation about the origin as shown in Figure 1.8. The corresponding displacements of any given particle are seen from the figure to be

$$u_x = -X - Y; \quad (1.17a)$$

$$u_y = X - Y; \quad (1.17b)$$

and therefore the application of the above formulas gives

$$\varepsilon_{xx} = \varepsilon_{yy} = -1; \quad \varepsilon_{xy} = 0. \quad (1.18a,b)$$

These values are clearly incorrect, as the solid experiences no strain during the rotation.